about how and when the Earth formed. Applying the tools of geochemistry to meteorites can provide the answer to this question. We close the chapter by attempting to construct a history of solar system and planetary formation from the meteorite record.

10.2 IN THE BEGINNING . . . NUCLEOSYNTHESIS

10.2.1 Astronomical background

Nucleosynthesis is the process of creation of the elements. While we could simply take for granted the existence of the elements, such an approach is somehow intellectually unsatisfactory. The origin of the elements is both a geochemical and astronomical question, perhaps even more a cosmological one. Our understanding of nucleosynthesis comes from a combination of observations of the abundances of the elements (and their isotopes) in meteorites and from observations of stars and related objects. Thus to understand how the elements formed, we need to understand a few astronomical observations and concepts. The universe began about 14 Ga ago with the Big Bang; since then the universe has been expanding, cooling, and evolving. This hypothesis follows from two observations: the relationship between red-shift and distance, and the cosmic background radiation, but particularly the former.

Stars shine because of exothermic nuclear reactions occurring in their cores. The energy released by these processes creates a tendency for thermal expansion that, in general, exactly balances the tendency for gravitational collapse. Surface temperatures are very much cooler than temperatures in stellar cores. For example, the Sun, which is an average star in almost every respect, has a surface temperature of 5700 K and a core temperature thought to be 14,000,000 K.

Stars are classified based on their color (and spectral emission lines), which is in turn related to their surface temperature. From hot to cold, the classification is: O, B, F, G, K, M, with subclasses designated by numbers, such as F5. (The mnemonic is "*O Be a Fine Girl, Kiss Me!*".) The Sun is class G. Stars are also divided into Populations. Population I stars are second or later generation stars and have greater heavy element contents than Population II stars. Population I stars are generally located in the main disk of the galaxy, whereas the old first-generation stars of Population II occur mainly in globular clusters that circle the main disk.

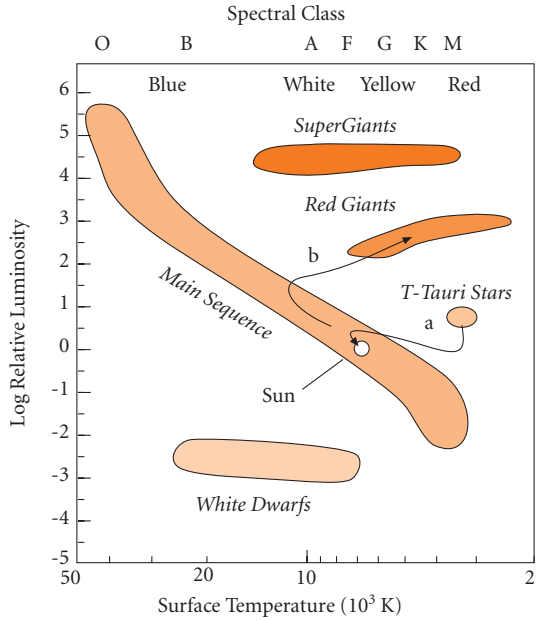

Figure 10.1 The Hertzsprung-Russell diagram of the relationship between luminosity and surface temperature. Arrows show the evolutionary path for a star the size of the Sun in pre- (a) and post- (b) main sequence phases.

On a plot of luminosity versus wavelength of their principal emissions (i.e., color), called a Hertzsprung-Russell diagram (Figure 10.1), most stars (about 90%) fall along an array defining an inverse correlation, called the "main sequence", between these two properties. Since wavelength is inversely related to the fourth power of temperature, this correlation means simply that hot stars give off more energy (are more luminous) than cooler stars. Mass and radius are also simply related to temperature for these so-called main sequence stars: hot stars are big, cool stars are small. Thus O and B stars are large, luminous and hot; K and M stars are small, faint, and cool. The relationship between mass, luminosity, and temperature is nonlinear, however. For example, an O star that is 30 times as massive as the Sun will have a surface temperature 7 times as hot and a luminosity 100,000 times

brighter. Stars on the main sequence produce energy by "hydrogen burning", fusion of hydrogen to produce helium. Since the rate at which this reaction occurs depends on temperature and density, hot, massive stars release more energy than smaller ones. As a result they exhaust the hydrogen in their cores much more rapidly. Thus there is an inverse relationship between the lifetime of a star, or at least the time it spends on the main sequence, and its mass. The most massive stars, up to 100 solar masses, have life expectancies of only about 10^6 years, whereas small stars, as small as 0.01 solar masses, remain on the main sequence for more than 10^{10} years.

The two most important exceptions to the main sequence stars, the red giants and the white dwarfs, represent stars that have burned all the H fuel in the cores and have moved on in the evolutionary sequence. H in the core is not replenished because the density difference prevents convection between the core and outer layers, which are still H-rich. The interior part of the core collapses under gravity. With enough collapse, the layer immediately above the He core will begin to "burn" H again, which again stabilizes the star. The core, however, continues to collapse until temperature and pressure are great enough for He burning to begin. At the same time, and for reasons not fully understood, the exterior expands and cools, resulting in a *red giant*, a star that is overluminous relative to main sequence stars of the same color. When the Sun reaches this phase, in perhaps another 5 Ga, it will expand to the Earth's orbit. A star will remain in the red giant phase for something like 10^6–10^8 years. During this time, radiation pressure results in a greatly enhanced solar wind, of the order of 10^{-6} to 10^{-7}, or even 10^{-4}, solar masses per year (the Sun's solar wind is 10^{-14} solar masses per year, so that in its entire lifetime the Sun will blow off 1/10,000 of its mass through the solar wind).

The fate of stars after the red giant phase (when the He in the core is exhausted) depends on their mass. Nuclear reactions in small stars cease and they simply contract, their exteriors heating up as they do so, to become *white dwarfs*. The energy released is that produced by previous nuclear reactions and gravitational potential energy. This is the likely fate of the Sun. White dwarfs are underluminous relative to stars of similar color on the main sequence. They can be thought of as little more than glowing ashes. Unless they blow off sufficient mass during the red giant phase, large stars die explosively, in supernovae. (Novae are entirely different events that occur in binary systems when mass from a main sequence star is pulled by gravity onto a white dwarf companion.) Supernovae are incredibly energetic events. The energy released by a supernova can exceed that released by an entire galaxy (which, it will be recalled, consists of on the order of 10^9 stars) for days or weeks!

10.2.2 The polygenetic hypothesis of Burbidge, Burbidge, Fowler and Hoyle

Our understanding of nucleosynthesis comes from three sets of observations: (1) the abundance of isotopes and elements in the cosmos; (2) experiments on nuclear reactions that determine what reactions are possible (or probable) under given conditions; and (3) inferences about possible sites of nucleosynthesis and about the conditions that prevail in those sites. The abundances of the elements in primitive meteorites are by far our most important source of information. Some additional information can be obtained from spectral observations of stars. The abundances of the elements in the solar system are shown in Figure 10.2. Any successful theory of nuclear synthesis must explain this abundance pattern. Thus the chemical and isotopic composition of meteorites is a matter of keen interest, not only to geochemists, but to astronomers and physicists as well.

The cosmology outlined earlier provides two possibilities for formation of the elements: (1) they were formed in the Big Bang itself, or (2) they were subsequently produced. One key piece of evidence comes from looking back into the history of the cosmos. Astronomy is a bit like geology in that just as we learn about the evolution of the Earth by examining old rocks, we can learn about the evolution of the cosmos by looking at old stars. The old stars of Population II are considerably poorer in heavy elements than are young stars. In particular, Population II stars have a Fe/H ratio typically a factor of 100 lower than the Sun. This suggests that much of the heavy element inventory of the galaxy has been produced since these stars formed

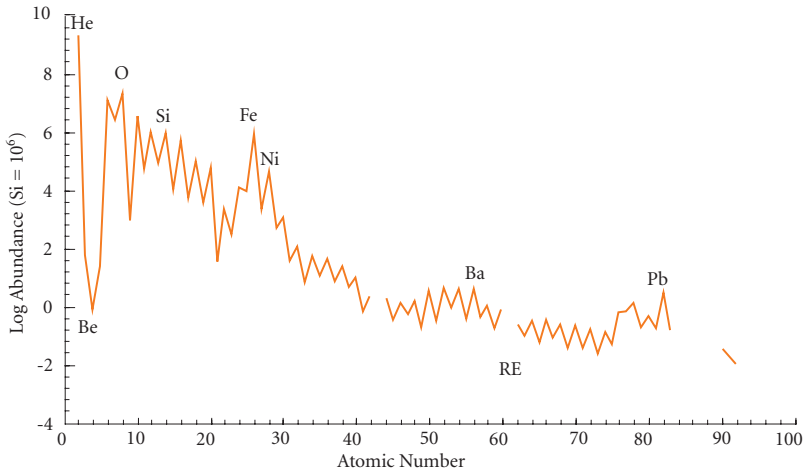

Figure 10.2 Solar system abundance of the elements relative to silicon as a function of atomic number.

more than 10 Ga ago. There are also significant variations in the Fe/H ratio between galaxies. In particular, dwarf spheroidal galaxies appear to be deficient in Fe, and sometimes in C, N, and O, relative to our own galaxy. Other galaxies show distinct radial compositional variations. For example, the O/H ratio in the interstellar gas of the disk of the spiral galaxy M81 falls by an order of magnitude with distance from the center. Finally, one sees a systematic decrease in the Fe/H ratio of white dwarfs (the remnants of small to medium size stars) with increasing age. On the other hand, old stars seem to have about the same He/H ratio as young stars. Indeed, ^{4}He seems to have an abundance of 25 ± 2% everywhere in the universe.

Thus the observational evidence suggests that (1) H and He are everywhere uniform, implying their creation and fixing of the He/H ratio in the Big Bang, and (2) elements heavier than Li were created by subsequent processes. The production of these heavier elements seems to have occurred steadily through time, but the efficiency of the process varies between galaxies and even within galaxies.

Early attempts (~1930–1950) to understand nucleosynthesis focused on single mechanisms. Failure to find a single mechanism that could explain the observed abundance of nuclides, even under varying conditions, led to the present view that relies on a number of mechanisms operating in different environments and at different times for creation of the elements in their observed abundances. This view, which has been called the polygenetic hypothesis, was first proposed by Burbidge, Burbidge, Fowler and Hoyle (1957). The abundance of trace elements and their isotopic compositions in meteorites were perhaps the most critical observations in development of the theory. An objection to the polygenetic hypothesis was the apparent uniformity of the isotopic composition of the elements, but variations in the isotopic composition have now been demonstrated for a few elements in some meteorites. The isotopic compositions of other elements, such as oxygen and the rare gases, vary between classes of almost all meteorites. Furthermore, there are significant variations in isotopic composition of some elements, such as carbon, among stars. These observations provide strong support for this theory.

To briefly summarize it, the polygenetic hypothesis proposes four phases of nucleosynthesis. *Cosmological nucleosynthesis* occurred shortly after the universe began and is responsible for the cosmic inventory of H and He, and some of the Li. Even though helium is the main product of nucleosynthesis in the interiors of main sequence stars, not enough helium has been produced in this manner to significantly change its cosmic abundance. The lighter elements, up to and including Si and a fraction of the heavier elements, but excluding Li and Be, are synthesized in the interiors of larger stars during the

final stages of their evolution (*stellar nucleosynthesis*). The synthesis of the remaining elements occurs as large stars exhaust the nuclear fuel in their interiors and explode in nature's grandest spectacle, the supernova (*explosive nucleosynthesis*). Finally, Li, B, and Be are continually produced in interstellar space by interaction of cosmic rays with matter (*galactic nucleosynthesis*).

10.2.3 Cosmological nucleosynthesis

Immediately after the Big Bang, the universe was too hot for any matter to exist. But within a microsecond or so, it had cooled to 10^{11} K so that matter began to condense. At first electrons, positrons, and neutrinos dominated, but as the universe cooled and expanded, protons and neutrons became more abundant. These existed in an equilibrium dictated by the following reactions:

$$^1\mathrm{H} + \mathrm{e}^- \rightleftharpoons \mathrm{n} + \nu$$

and

$$\mathrm{n} + \mathrm{e}^+ \rightleftharpoons {}^1\mathrm{H} + \bar{\nu}\ ^*$$

At first, neutrons and protons existed in equal numbers. But as temperatures cooled through 10^{10} K, the reactions above progressively favored protons. These reactions are possible only at these extreme temperatures, so that in less than two seconds they ceased, freezing in a 6 to 1 ratio of protons to neutrons.

A somewhat worrisome question is why matter exists at all. Symmetry would seem to require production of equal numbers of protons and anti-protons that would have annihilated themselves by:

$$\mathrm{p} + \bar{\mathrm{p}} \rightarrow 2\gamma^\dagger$$

The current theory is that the hyperweak force was responsible for an imbalance favoring matter over anti-matter. The same theory predicts a half-life of the proton of 10^{32} yrs, a prediction not yet verified.

It took another 100 seconds for the universe to cool to 10^9 K, which is cool enough for ^{2}H to form:

$$^1\mathrm{H} + {}^1\mathrm{n} \rightarrow {}^2\mathrm{H} + \gamma$$

At about the same time, the following reactions could also occur:

$$^2\mathrm{H} + {}^1\mathrm{n} \rightarrow {}^3\mathrm{H} + \gamma; \quad {}^2\mathrm{H} + {}^1\mathrm{H} \rightarrow {}^3\mathrm{H} + \gamma$$

$$^2\mathrm{H} + {}^1\mathrm{H} \rightarrow {}^3\mathrm{He} + \beta^+ + \gamma; \quad {}^3\mathrm{He} + \mathrm{n} \rightarrow {}^4\mathrm{He} + \gamma$$

and

$$^2\mathrm{H} + {}^2\mathrm{H} \rightarrow {}^3\mathrm{He} + \mathrm{n}; \quad {}^3\mathrm{He} + {}^4\mathrm{He} \rightarrow {}^7\mathrm{Be} + \gamma;$$

$$^7\mathrm{Be} + \mathrm{e}^- \rightarrow {}^7\mathrm{Li} + \gamma$$

Formation of elements heavier than Li, however, was inhibited by the instability of nuclei of masses 5 and 8. Figure 10.3 illustrates the compositional evolution of the early cosmos. Two factors bring this process to a halt: (1) falling temperatures and (2) the decay of free neutrons: outside the nucleus, neutrons have a half-life of only 10 minutes, so nucleosynthetic reactions that consume neutrons eventually cease. Within 20 minutes or so, the universe cooled below 3×10^8 K and nuclear reactions were no longer possible. Thus, the Big Bang created H, He, and Li (^{7}Li/H = 10^{-9}). Some 400,000 years later, the universe had cooled to about 3000 K, cool enough for electrons to be bound to nuclei, forming atoms. With this *recombination*, the universe became transparent, that is, radiation could freely propagate through it. The faint radiation known as the cosmic background radiation provides a snapshot of the universe at that time.

The first seconds and minutes of the cosmos are surprisingly well understood, in part because the conditions that prevailed can be reproduced, at least on a micro-scale, in high-energy accelerators/colliders. Experiments in these accelerators provide tests and calibrations of cosmological theory. The ratios of hydrogen, helium, and lithium created by these reactions depend upon density and temperature and, in part because of the decay of free neutrons, they are also a function of the rate at which these fall as the cosmos expands. An indication of the success of cosmological theory is that it predicts the H and He abundances, and their isotopic composition, in the cosmos. On the other hand, the very earliest

* The ν (nu) is the symbol for a neutrino; the bar indicates the anti-particle, an anti-neutrino in this case.
† γ (gamma) is used here to indicate energy in the form of a gamma ray.

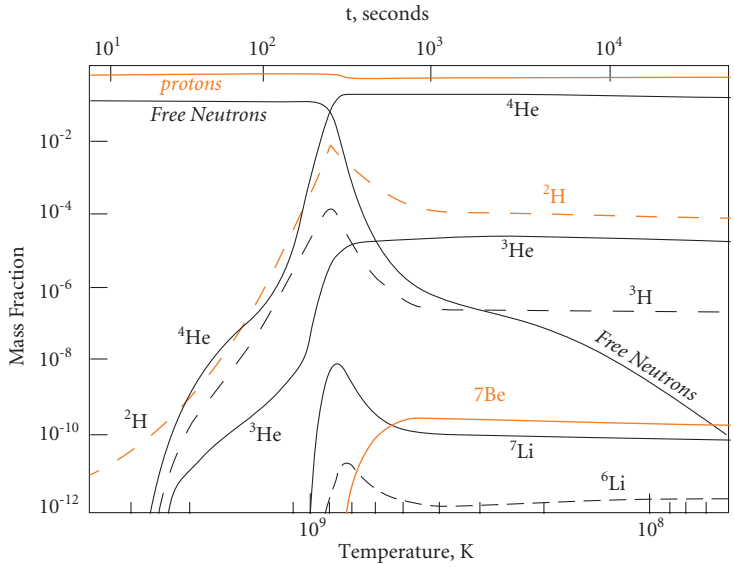

Figure 10.3 Compositional evolution during cosmological nucleosynthesis. ^{7}Be and ^{3}H are unstable and decay to ^{7}Li and ^{3}He with half-lives of 53 days (4.6×10^{6} s) and 12.3 years (4×10^{8} s) respectively. After Ned Wright's Cosmology Tutorial (http://www.astro.ucla.edu/~wright/cosmolog.htm).

history of the cosmos, the first femtosecond or so, is less well understood because the conditions that prevailed are too energetic to be reproduced in accelerators.

10.2.4 Nucleosynthesis in stellar interiors

10.2.4.1 Hydrogen, helium, and carbon burning stars

For quite some time after the Big Bang, the universe was a more or less homogenous, hot gas. "Less" turns out to be critical. Inevitably (according to fluid dynamics), inhomogeneities developed in the gas, and indeed, very slight inhomogeneities are observed in the cosmic background radiation. These inhomogeneities enlarged in a sort of runaway process of gravitational attraction and collapse. Thus were formed protogalaxies, perhaps 0.5 Ga after the Big Bang. Instabilities within the protogalaxies collapsed into stars. Once this collapse proceeded to the point where density reached 6 g/cm and temperature reached 10 to 20 million K, nucleosynthesis began in the interior of stars by *hydrogen burning*, or the *pp process*, which involves reactions such as:

$$^{1}H + {}^{1}H \rightarrow {}^{2}H + \beta^{+} + \nu; \quad {}^{2}H + {}^{1}H \rightarrow {}^{3}He + \gamma$$

and

$$^{3}He + {}^{3}He \rightarrow {}^{4}He + 2{}^{1}H + \gamma$$

There are also other reaction chains that produce ^{4}He which involve Li, Be, and B, either as primary fuel or as intermediate reaction products. Later, when some carbon had already been produced by the first generation of stars and supernovae, second and subsequent generation stars with masses greater than about 1.1 solar masses produced He by another process as well, the *CNO cycle*:

$$^{12}C(p, \gamma)\ ^{13}N(\beta^{+}, \gamma)\ ^{13}C(p, \gamma)\ ^{14}N(p, \gamma)$$
$$^{15}O(\beta^{+}, \nu)\ ^{15}N(p, \alpha)\ ^{12}C^{*}$$

* Here we are using a notation commonly used in nuclear physics. The notation:

$$^{12}C(p, \gamma)^{13}N$$

is equivalent to:

$$^{12}C + p \rightarrow {}^{13}N + \gamma$$

In this process, carbon acts as a sort of nuclear catalyst: it is neither produced nor consumed. The net effect is consumption of 4 protons and 2 positrons to produce a neutrino, some energy and a ^{4}He nucleus. The $^{14}N(p,\gamma)^{15}O$ is the slowest in this reaction chain, so there tends to be a net production of ^{14}N as a result. Also, though both ^{12}C and ^{13}C are consumed in this reaction, ^{12}C is consumed more rapidly, so this reaction chain should increase the $^{13}C/^{12}C$ ratio.

The heat produced by these reactions counterbalances gravitational collapse and these reactions proceed in main sequence stars (Figure 10.1) until the hydrogen in the stellar core is consumed. How quickly this happens depends, as we noted earlier, on the mass of the star.

Once the H is exhausted in the stellar core, fusion ceases, and the balance between gravitational collapse and thermal expansion is broken. The interior of the star thus collapses, raising the star's temperature. The exterior expands and fusion begins in the shells surrounding the core, which now consists of He. This is the *red giant* phase. If the star is massive enough for temperatures to reach 10^{8} K and density to reach 10^{4} g/cc in the He core (stars with masses greater than about 0.8 solar masses), *He burning* can occur:

$$^{4}He + {}^{4}He \rightarrow {}^{8}Be + \gamma$$

and

$$^{8}Be + {}^{4}He \rightarrow {}^{12}C + \gamma$$

The catch in this reaction is that the half-life of ^{8}Be is only 10^{-16} sec, so 3 He nuclei must collide essentially simultaneously, hence densities must be very high. He burning also produces O, and lesser amounts of ^{20}Ne and ^{24}Mg, in the red giant phase, but Li, Be, and B are skipped: they are not synthesized in these phases of stellar evolution. These nuclei are unstable at the temperatures of stellar cores. Rather than being produced, they are consumed in stars.

There is a division of evolutionary paths once helium in the stellar core is consumed. Densities and temperatures necessary to initiate further nuclear reactions cannot be achieved by low-mass stars, such as the Sun (because the gravitational force is not sufficient to overcome coulomb repulsion of electrons), so their evolution ends after the Red Giant phase, the star becoming a white dwarf. Massive stars, those greater than about 4 $M_{\odot}$,* however, undergo further collapse and the initiation of *carbon and oxygen burning* when temperatures reach 600 million K and densities 5×10^{5} g/cc. However, stars with intermediate masses, between 4 and 11 $M_{\odot}$, can be entirely disrupted by the initiation of carbon burning. For stars more massive than 11 $M_{\odot}$, about 1% of all stars, evolution now proceeds at an exponentially increasing pace (Figure 10.4) with reactions of the type:

$$^{12}C + {}^{12}C \rightarrow {}^{20}Ne + {}^{4}He + \gamma$$

$$^{16}O + {}^{16}O \rightarrow {}^{28}Si + {}^{4}He + \gamma$$

and

$$^{12}C + {}^{16}O \rightarrow {}^{24}Mg + {}^{4}He + \gamma$$

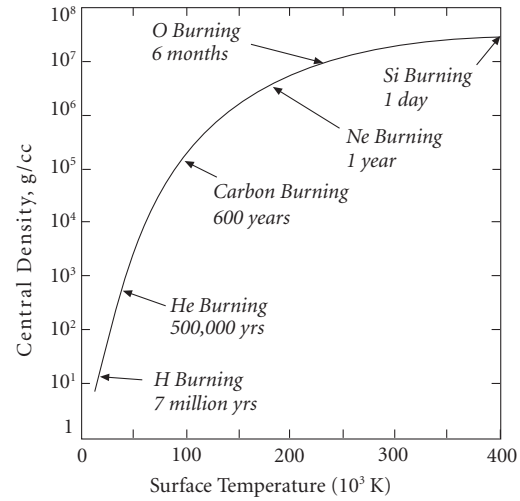

Figure 10.4 Evolutionary path of the core of star of 25 solar masses (adapted from Bethe and Brown, 1985). Note that the period spent in each phase depends on the mass of the star: massive stars evolve more rapidly.

* The symbol ⊙ is the astronomical symbol for the Sun. $M_{\odot}$ therefore indicates the mass of the Sun.

Also, ^{14}N created during the hydrogen-burning phase of second-generation stars can be converted to ^{22}Ne. A number of other less abundant nuclei, including Na, Al, P, S, and K are also synthesized at this time, and in the subsequent process, *Ne burning*.

During the final stages of evolution of massive stars, a significant fraction of the energy released is carried off by neutrinos created by electron–positron annihilations in the core of the star. If the star is sufficiently oxygen-poor that its outer shells are reasonably transparent, the outer shell of the red giant may collapse during last few 10^4 years of evolution to form a *blue giant*.

10.2.4.2 The e-process

Eventually, a new core consisting mainly of ^{28}Si is produced. At temperatures near 10^9 K and densities above 10^7 g/cc a process known as *silicon burning*, or the *e-process* (for equilibrium), begins, and lasts for a week or less, again depending on the mass of the star. The process of silicon burning is really a variety of reactions that can be summarized as the photonuclear rearrangement of a gas originally consisting of ^{28}Si nuclei into one which, via intervening beta decays, consists mainly of ^{56}Ni, which then decays with a half-life of 6 days to ^{56}Fe, the most stable of all nuclei. At 10^9 K, thermal photons have energies near 1 MeV; absorbing such photons overcomes the energy barriers between nuclei, allowing the system to evolve towards a minimum energy state by making the most stable nuclei. This is analogous to the rapid approach to chemical equilibrium that occurs once temperatures become high enough to overcome kinetic barriers.

The e-process includes reactions such as:

$$^{28}Si + \gamma \rightleftharpoons {}^{24}Ne + {}^{4}He$$
$$^{28}Si + {}^{4}He \rightleftharpoons {}^{32}S + \gamma$$
$$^{32}S + {}^{4}He \rightleftharpoons {}^{36}Ar + \gamma$$

While these reactions can proceed in either direction, there is a tendency for the build-up of heavier nuclei with masses 32, 36, 40, 44, 48, 52, and 56. Partly as a result of the e-process, these nuclei are unusually abundant in nature. In addition, because a variety of nuclei are produced during C and Si burning phases, other reactions are possible, synthesizing a number of minor nuclei.

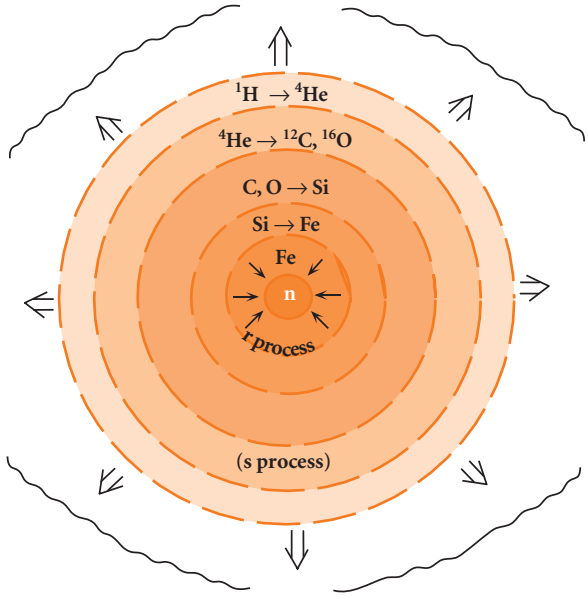

Figure 10.5 Schematic diagram of stellar structure at the onset of the supernova stage. Nuclear burning processes are illustrated for each stage.

The star is now a cosmic onion of sorts, consisting of a series of shells of successively heavier nuclei and a core of Fe (Figure 10.5). Though temperature increases toward the interior of the star, the structure is stabilized with respective to convection and mixing because each shell is denser than the one overlying it.

Fe-group elements may also be synthesized by the e-process in Type I supernovae.* Type I supernovae occur when white dwarfs of intermediate mass (3–10 solar masses) in binary systems accrete material from their companion. When their cores reach the so-called Chandrasekhar limit, C burning is initiated and the star explodes.

* Astronomers recognize two kinds of supernovae: Type I and Type II. The explosions of massive stars that we are considering are the Type II supernovae.

10.2.4.3 *The s-process*

In second and later generation stars containing heavy elements, yet another nucleosynthetic process can operate. This is the slow neutron capture or *s-process*. It is so called because the rate of capture of neutrons is slow compared with the *r-process*, which we will discuss later. It operates mainly in the red giant phase (as evidenced by the existence of ^{99}Tc and enhanced abundances of several s-process nuclides in red giants) where neutrons are produced by reactions such as:

$$^{13}\mathrm{C} + {}^{4}\mathrm{He} \rightarrow {}^{16}\mathrm{O} + \mathrm{n}$$
$$^{22}\mathrm{Ne} + {}^{4}\mathrm{He} \rightarrow {}^{25}\mathrm{Mg} + \mathrm{n}$$
$$^{17}\mathrm{O} + {}^{4}\mathrm{He} \rightarrow {}^{20}\mathrm{Ne} + \mathrm{n}$$

(but even H burning produces neutrons, so that the s-process operates to some degree even in main sequence stars). These neutrons are captured by nuclei to produce successively heavier elements. The principal difference between the s-process and r-process, discussed later, is the rate of capture relative to the decay of unstable isotopes. In the s-process, a nucleus may only capture a neutron every thousand years or so. If the newly produced nucleus is not stable, it will decay before another neutron is captured. As a result, the s-process path closely follows the valley of stability on the chart of the nuclides and nuclear instabilities cannot be bridged.

10.2.5 Explosive nucleosynthesis

The e-process stops at mass 56. In Chapter 8 we noted that ^{56}Fe had the highest binding energy per nucleon, that is, it is the most stable nucleus. Thus fusion can release energy only up to mass 56; beyond this the reactions become endothermic and consume energy. Once the stellar core has been largely converted to Fe, a critical phase is reached: the balance between thermal expansion and gravitational collapse is broken. The stage is now set for the catastrophic death of the star: a supernova explosion, the ultimate fate of stars with masses greater than about 8 solar masses. The energy released in the supernova is astounding. In its first 10 seconds, the 1987A supernova (Figure 10.6) released more energy than the entire visible universe, and 100 times more energy than the Sun will release in its entire 10 billion year lifetime.

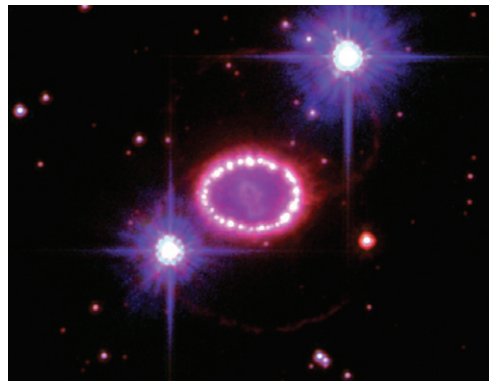

Figure 10.6 Rings of glowing gas surrounding the site of the supernova explosion named Supernova 1987A photographed by the wide field planetary camera on the Hubble Space Telescope in 1994. The nature of the rings is uncertain, but they may be debris of the supernova illuminated by high-energy beams of radiation or particles originating from the supernova remnant in the center. Image: NASA.

When the mass of the iron core reaches 1.4 solar masses (the Chandrasekhar mass), further gravitational collapse cannot be resisted even by coulomb repulsion. The supernova begins with the collapse of this stellar core, which would have a radius of several thousand km (similar to the Earth's radius) before collapse, to a radius of 100 km or so. The collapse occurs in a few tenths of a second. When matter in the center of the core is compressed beyond the density of nuclear matter (3×10^{14} g/cc), it rebounds, sending a massive shock wave back out. As the shock wave travels outward through the core, the temperature increase resulting from the compression produces a breakdown of nuclei by photodisintegration, for example:

$$^{56}\mathrm{Fe} + \gamma \rightarrow 13\ {}^{4}\mathrm{He} + 4\ {}^{1}\mathrm{n};$$
$$^{4}\mathrm{He} + \gamma \rightarrow 2\ {}^{1}\mathrm{H} + 2\ {}^{1}\mathrm{n}$$

Thus much of what took millions of years to produce is undone in an instant. However, photodisintegration produces a large number of free neutrons (and protons), which leads to another important nucleosynthetic process, the *r-process*.

Another important effect is the creation of huge numbers of neutrinos by positron–electron annihilations, these particles having "condensed" as pairs from gamma rays. The energy carried away by neutrinos leaving the supernova exceeds the kinetic energy of the explosion by a factor of several hundred, and exceeds the visible radiation by a factor of some 30,000. The neutrinos leave the core at nearly the speed of light. Though neutrinos interact with matter very weakly, the density of the core is such that their departure is delayed slightly. Nevertheless, they travel faster than the shock wave and are delayed less than electromagnetic radiation. Thus neutrinos from the 1987A supernova arrived at Earth (some 160,000 years after the event) a few hours before the supernova became visible.

When the shock wave reaches the surface of the core, the outer part of the star is blown apart in an explosion of unimaginable violence. But amidst the destruction, new nucleosynthetic processes occur. As the shock wave passes through outer layers, it may "reignite" them, producing explosive Ne, O, and C burning. These processes produce isotopes of S, Cl, Ar, Ca, Ti, and Cr, and some Fe.

10.2.5.1 The r-process

The neutrons produced by photodisintegration in the core are captured by those nuclei that manage to survive this hell. Because the abundance of neutrons is exceedingly high, nuclei capture them at a rapid rate – so rapid that even an unstable nucleus will capture a neutron before it has an opportunity to decay. The result is a build-up of neutron-rich unstable nuclei. Eventually the nuclei capture enough neutrons that they are not stable even for a small fraction of a second. At that point, they undergo β^- decay to new nuclides, which are more stable and capable of capturing more neutrons. This is the *r-process* (rapid neutron capture), and is the principal mechanism for building up the heavier nuclei. It reaches a limit when nuclei beyond A ≈ 90 are reached. These heavy nuclei fission into several lighter fragments. The r-process is thought to have a duration of 1 to 100 sec during the peak of the supernova explosion. Figure 10.7 illustrates this process.

The r-process produces broad peaks in elemental abundance around the neutron magic numbers (50, 82, 126, corresponding to the elements Sr and Zr, Ba, and Pb). This occurs because nuclei with magic numbers of

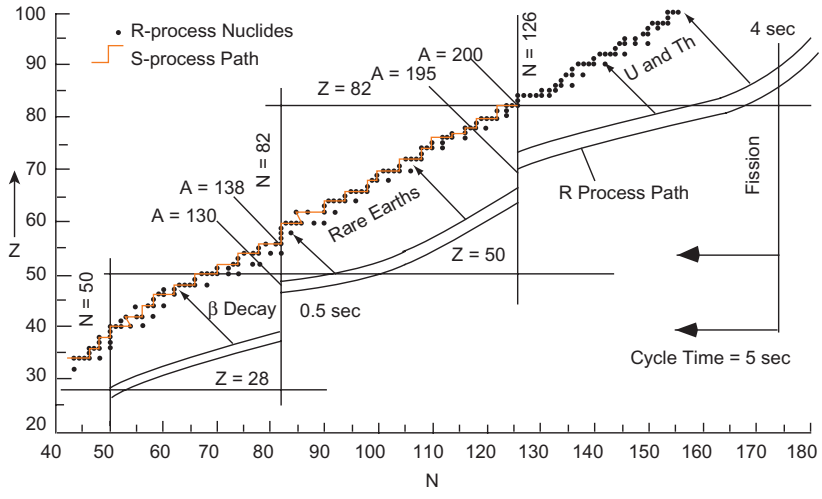

Figure 10.7 Diagram of the r-process path on a Z versus N diagram. The r-process path is indicated; the solid line through stable isotopes shows the s-process path.

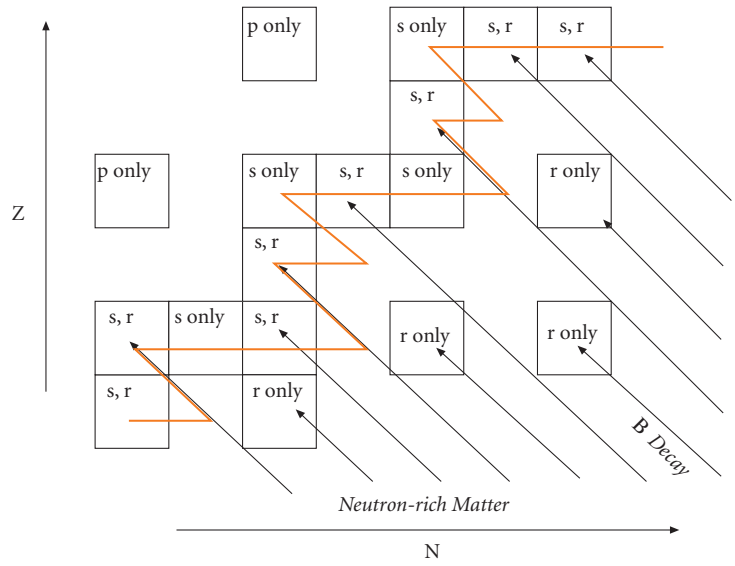

Figure 10.8 Z versus N diagram showing production of isotopes by the r-, s- and p-processes. Squares are stable nuclei; wavy lines are the beta-decay path of neutron-rich isotopes produced by the r-process; a solid line through stable isotopes shows the s-process path.

neutrons are particularly stable, have very low cross-sections for capture of neutrons, and because nuclei just short of magic numbers have particularly high capture cross-sections. Thus the magic number nuclei are both created more rapidly and destroyed more slowly than other nuclei. When they decay, the sharp abundance peak at the magic number becomes smeared out.

10.2.5.2 The p-process

The r-process tends to form the heavier (neutron-rich) isotopes of a given element. Proton capture, or the *p-process*, also occurs in supernovae and is responsible for the lightest isotopes of a given element. The probability of proton capture is much less than that of neutron capture. You can easily imagine the reason for this: to be captured, the proton must have sufficient energy to overcome the coulomb repulsion and approach to within 10^{-14} cm of the nucleus where the strong force dominates over the electromagnetic one. In contrast, even low-energy neutrons can be captured by nuclei since the neutron is uncharged and there is no coulomb repulsion. The production of nuclei by the p-process is much less than by neutron capture processes, and is significant only for those nuclides that cannot be produced in other ways. These tend to be the lightest isotopes of an element. Because of the improbability of proton capture, these light, p-process-only isotopes tend to be the least abundant.

Figure 10.8 illustrates how these three processes, the s-, r-, and p-processes, create different nuclei. Notice the shielding effect. If an isotope with z protons and n neutrons has a stable isobar with $n + x$ neutrons and $p - x$ protons, this isotope is shielded from production by the r-process because β-decay will cease when that stable isobar is reached. The most abundant isotopes of an element tend to be those created by all processes; the least abundant are those created by only one, particularly by only the p-process. The exact abundance of an isotope depends on a number of factors, including its neutron-capture cross-section,* and the neutron-capture cross-section and stability of neighboring nuclei.

* In a given flux of neutrons, some nuclides will be more likely to capture and bind a neutron than others, just as some atoms will be more likely to capture and bind an electron than others. The neutron-capture cross-section of a nuclide is a measure of the affinity of that nuclide for neutrons, i.e., a measure of the probability of that nuclide capturing a neutron in a given neutron flux.

Let's return to the exploding star. In the inner part of the stellar core, the reactions we just discussed do not take place. Instead, the core collapses to the point where all electrons are welded to protons to form a ball of neutrons: a neutron star. This inner core is hot: 100 billion kelvin. And like a ballerina pulling in her arms, it conserves angular momentum by spinning faster as it collapses. The neutron star inside the expanding supernova shell of 1987A may be spinning at 2000 revolutions per second. Neutron stars emits radiation in beacon-like fashion: a *pulsar*. The collapse of cores of the most massive stars, however, may not stop at all. They collapse to a diameter of zero and their density becomes infinite. Such an object is called a singularity. Its gravitational attraction is so great even light cannot escape, creating a *black hole*.

10.2.6 Nucleosynthesis in interstellar space

Except for production of ^{7}Li in the Big Bang, Li, Be, and B are not produced in any of the earlier situations. One clue to the creation of these elements is their abundance in galactic cosmic rays: they are overabundant by a factor of 10^{6}, as is illustrated in Figure 10.9. They are believed to be formed by interactions of cosmic rays with interstellar gas and dust, primarily reactions of ^{1}H and ^{4}He with carbon, nitrogen and oxygen nuclei. These reactions occur at high energies (higher than the Big Bang and stellar interiors), but at low temperatures where the Li, B and Be can survive.

10.2.7 Summary

Figure 10.10 is a part of the Z versus N plot showing the abundance of the isotopes of elements 68 through 73. It is a useful region of the chart of the nuclides for illustrating how

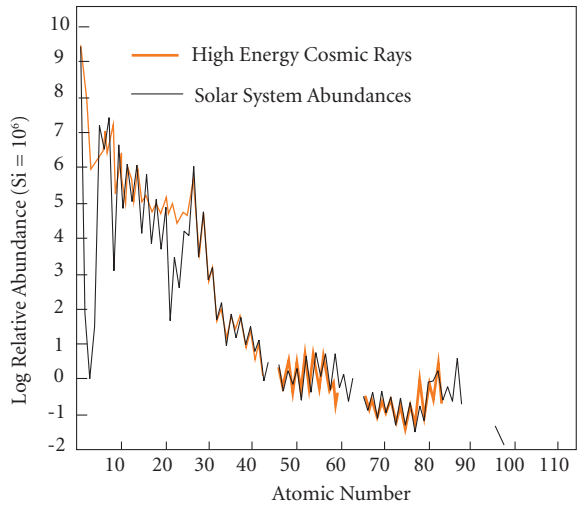

Figure 10.9 Comparison of relative abundances in cosmic rays and the solar system.

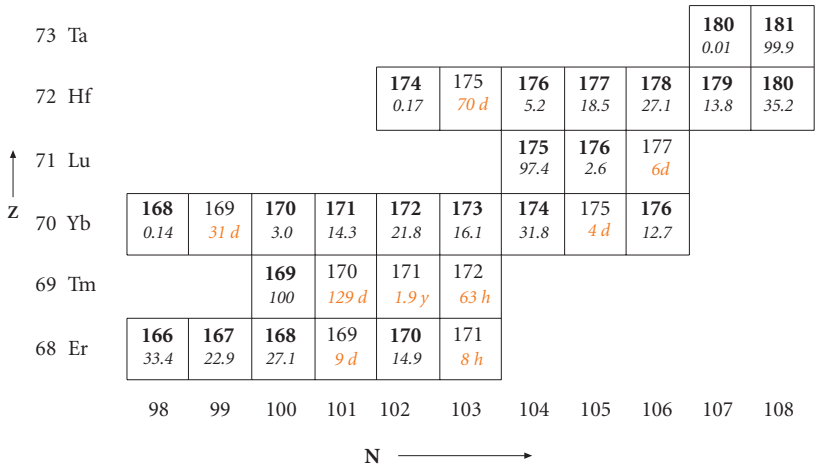

Figure 10.10 View of part of the chart of the nuclides. Mass numbers of stable nuclides are shown in bold, their isotopic abundance is shown in italics as percent. Mass numbers of short-lived nuclides are shown in red plain text with their half-lives also given.

the various nucleosynthetic processes have combined to produce the observed abundances. First, we notice that even-numbered elements tend to have more stable nuclei than odd-numbered ones – a result of the greater stability of nuclides with even Z. We also notice that nuclides having a neutron-rich isobar (recall that isobars have the same value of A, but a different combination of N and Z) are underabundant, for example ^{170}Yb and ^{176}Lu. This under-abundance results from these nuclides being "shielded" from production by β^- decay of r-process neutron-rich nuclides. In these two examples, ^{170}Er and ^{176}Yb would be the ultimate product of neutron-rich unstable nuclides of mass number 170 and 176 produced during the r-process. Also notice that ^{168}Yb, ^{174}Hf and ^{180}Ta are very rare. These nuclides are shielded from the r-process and are also off the s-process path. They are produced only by the p-process. Finally, those nuclides that can be produced by both the s-process and the r-process tend to be the most abundant; for example, ^{176}Yb is about half as abundant as ^{174}Yb because the former is produced by the r-process only while the latter can be produced by both the s-process and the r-process. ^{176}Yb cannot be produced by the s-process because during the s-process, the flux of neutrons is sufficiently low that any ^{175}Yb produced decays to ^{175}Lu before it can capture a neutron and become a stable ^{176}Yb.

The heavy element yield of stellar and explosive nucleosynthesis will vary tremendously with the mass of the star. A star of 60 solar masses will convert some 40% of its mass to heavy elements. The bulk of this is apparently ejected into the interstellar medium. Stars too small to become supernovae will convert relatively small fractions of their mass to heavy elements, and only a very small fraction of this will be ejected. On the whole, stars in the mass range of 20–30 solar masses probably produce the bulk of the heavy elements in the galaxy. While such stars, which are already quite large compared with the mean stellar mass, convert a smaller fraction of their mass to heavy elements than truly massive stars, they are much more abundant.

Novae may also make a significant contribution to the cosmic inventory of a few relatively light elements such as ^{19}F and ^{7}Li, as well as the rarer isotopes of C, N, and O. Novae occur when mass is accreted to a white dwarf from a companion red giant. If the material is mainly hydrogen and accretion is relatively slow, H burning may be ignited on the surface of the white dwarf, resulting in an explosion that ejects a relatively small fraction of the mass of the star.

10.3 METEORITES: ESSENTIAL CLUES TO THE BEGINNING

In subsequent sections we want to consider the formation of the Earth and its earliest history. The Earth is a dynamic body; its rock formations are continually being recycled into new ones. As a result, old rocks are rare. The oldest rocks are 4.0 Ga; some zircon grains as old as 4.4 Ga have been found in coarse-grained, metamorphosed sediments. The geologic record ends there: there is no trace of the earliest history of the Earth in terrestrial rocks. So to unravel Earth's early history, we have to turn to other bodies in the solar system. So far, we have samples only of the Moon and meteorites, and a few analyses of the surface of Venus and Mars.* The Moon provides some clues to the early history of planets, but meteorites provide the best clues as to the formation of planets and the solar system. We now turn our attention to them.

Meteorites are traditionally classified according to their composition, mineralogy, and texture. The first-order division is between *stones* and *irons*. You can pretty well guess what this means: stones are composed mainly of silicates, while irons are mainly metal. An intermediate class is the *stony-irons*, a mixture of silicate and metal. Stones are subdivided into *chondrites* and *achondrites* depending on whether they contain *chondrules*, which are small spherical particles that were once molten and can constitute up to 80% of the mass of chondrites (though the average is closer to perhaps 40%).

Another way of classifying meteorites is to divide them into *primitive* and *differentiated*.

* As we shall see, a few meteorites probably come from Mars, providing additional information on the composition of that planet.

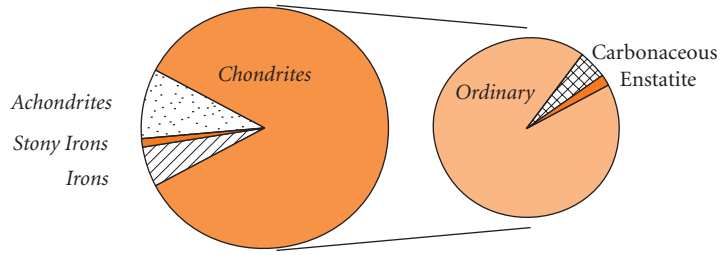

Figure 10.11 Relative abundance of major types of meteorites falls. The smaller pie chart on the right shows the relative proportions of different chondrite classes.

Chondrites constitute the primitive meteorites, while the achondrites, irons, and stony-irons constitute the differentiated meteorites. *The chemical and physical properties of chondrites are primarily a result of processes that occurred in the solar nebula*, the cloud of gas and dust from which the solar system formed. On the other hand, *the chemical and physical properties of differentiated meteorites are largely the result of igneous processes occurring on meteorite parent bodies, namely asteroids*. Primitive meteorites contain clues about early solar system formation, whereas differentiated meteorites contain clues about early planetary differentiation.

Meteorites are also divided into *falls* and *finds*. Falls are meteorites recovered after observation of a fireball whose trajectory can be associated an impact site. Finds are meteorites found but not observed falling. Some finds have been on the surface of the Earth for considerable time and consequently can be weathered. Thus the compositional information they provide is less reliable than that of falls. An exception of sorts to this is the Antarctic meteorites. Meteorites have been found in surprising numbers in the last 30 years or so in areas of low snowfall in Antarctica where ice is eroded by evaporation and wind. Meteorites are concentrated in such areas by glaciers. Because of storage in the Antarctic deep freeze, they are little weathered.

Figure 10.11 illustrates the relative abundance of the various meteorite types among falls. Stones, and ordinary chondrites in particular, predominate among falls. Irons are over-represented among finds because they are more likely to be recognized as meteorites, and because they are more likely to be preserved. Even among the falls, irons may be over-represented for these reasons. There are over 53,000 meteorites in collections around the world, most of which now come from Antarctic collecting programs and similar scientific collecting programs in the deserts of Africa and Australia.

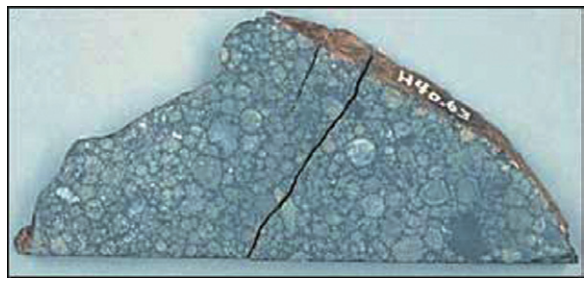

Figure 10.12 *Leoville* (CV3) carbonaceous chondrite. Many of the chondrules have been deformed into elongate spheroids. This meteorite also contains CAIs. Image: NASA.

10.3.1 Chondrites: the most primitive objects

Chondrites consist of varying proportions of the following: chondrules, refractory calcium-aluminum inclusions (generally called CAIs), amoeboid olivine aggregates (AOAs), and a fine-grained mixture of minerals and amorphous material called the matrix – we'll discuss these components in more detail later. An example is shown in Figure 10.12. The mineralogical, textural, and compositional (including isotopic composition) features of these components indicate that they formed while dispersed in the solar nebula and were subsequently aggregated to form the meteorite parent bodies. These components were subsequently processed in the parent bodies

through aqueous alteration or thermal metamorphism. In addition, many are highly brecciated as a result of collisions and impacts on the surface of the parent bodies. Nevertheless, most chondrite classes have concentrations of *condensable* elements, that is, all elements except H, C, N, O, and the noble gases, that are within a factor of 2 of solar concentrations. This contrasts strongly with the composition of differentiated meteorites, terrestrial materials, lunar materials, and so on, all of which differ strongly from the solar composition. Since the Sun comprises more than 99% of the mass of the solar system, its composition is effectively identical to the composition of the solar system, and to the solar nebula from which the solar system formed. *The importance of chondrites is thus clear: they represent samples of the cloud of gas and dust from which all bodies in the solar system formed.* To the degree that they have not been obscured by subsequent processing in asteroidal bodies, details of their compositions, their mineralogy, and their textures provide insights into the conditions and processes in the solar nebula that led to the solar system we observe and inhabit today.

10.3.1.1 Chondrite classes and their compositions

Table 10.1 summarizes the general characteristics of the various chondrite groups. There are three main classes: *Carbonaceous (C)*, *Ordinary,* and *Enstatite (E)* chondrites. The ordinary and E chondrites are further subdivided based on their iron and nickel content and the degree of oxidation of the iron. The *ordinary chondrites*, which as Figure 10.11 shows are by far the most common, are composed primarily of olivine, orthopyroxene and lesser amounts of Ni-Fe alloy. They are subdivided into classes H (high iron or bronzite), L (low iron or hypersthene), and LL. The name LL reflects low total iron and low metallic iron. H chondrites contain 25–31% total iron, of which 15–19% is reduced, metallic iron. L chondrites contain 20–25% iron, of which 4–10% is metallic. LL chondrites contain about the same total iron as L chondrites, but only 1–3% is metallic. The enstatite chondrites are highly reduced, with virtually all the iron present as metal. Reduction of iron increases the $Si/(Fe^{2+}+Mg)$ ratio in silicates and results in enstatite, rather than olivine, being the dominant mineral in these objects, hence the name of the class. The E chondrites can be further subdivided into EH (high iron) and EL (low iron) classes. Besides enstatite, metal and sulfides, enstatite chondrites contain a number of other exotic minerals, such as phosphides, carbides and a oxynitride of Si, that indicate they formed under highly reducing conditions.

The amount of Fe and the degree of oxidation are two of the features that differentiate the various chondrite classes. This is illustrated in Figure 10.13. The diagonal lines are lines of constant total iron content. H and C chondrites have similar total iron contents, but their oxidation state differs (carbonaceous chondrites are more oxidized). L and LL chondrites have lower total iron contents (and variable oxidation state). E chondrites are highly reduced, and may have high (EH) or low (EL) total iron. The variation in Fe content extends to other siderophile elements as well, reflecting general fractionation between siderophile and lithophile elements in the solar nebula.

As their name implies, *carbonaceous chondrites* differ from other chondrite classes in being rich in carbon compounds, including a variety of organic compounds, most notably amino acids (indeed, 70 different amino acids have been identified in *Murchison* – there are only 20 biological amino acids). They are also enriched in hydrogen (present mainly in hydrated silicates) and nitrogen and somewhat poorer in Si compared with other chondrites. The composition of carbonaceous chondrites matches that of the Sun even more closely than chondrites as a whole. They are subdivided into 8 subgroups, with the name of each subgroup derived from a type example: CI (*Ivuna*), CM (*Mighei*), CV (*Vigarano*) and CO (*Ornans*), CK (*Karoonda*), CR (*Renazzo*), CB (*Bencubbin*), CH (High Iron). Of these, meteorites from the CM, CV, and CO groups are the most common. CI chondrites are rare, but are nevertheless of great significance. Perhaps ironically, CI chondrites lack chondrules and CAIs. Nevertheless, they are rich in carbonaceous matter and are compositionally similar to other chondrites and hence classed with the carbonaceous chondrites. Table 10.2 lists the concentrations of the elements in the CI chondrite *Orgueil* and the solar photo-

Table 10.1 Characteristics of chondrite groups.

	Principal ferromagnesian silicate	RIs (vol. %)	Fe/(Fe+Mg) of silicate (mol %)	Metal (vol %)	Mean Mg/Si (molar)	Mean Al/Si (mol %)	Mean Ca/Si (mol %)	$\delta^{18}O$ ‰	$\delta^{17}O$ ‰	Chondrules	
										Size (mm)	Volume (%)
Carbonaceous											
CI	serpentine	<0.01	45	<0.01	1.05	8.6	6.2	16.4	8.8	–	–
CM	serpentine	5	43	0.1	1.05	9.7	6.8	12.2	4.0	0.3	20
CO	olivine	13	9–23	1–5	1.05	9.3	6.8	–1.1	–5.1	0.2	40
CV	olivine	10	6–14	0–5	1.07	11.6	8.4	0	–4.0	1.0	45
CK	olivine	4	29–33	<0.01	1.08	10.2	7.6	–0.8	–4.6	0.8	15
CR	chlorite	0.5	37–40	5–8	1.05	8.2	5.6	6.3	2.3	0.7	50–60
CH	olivine	0.1	2.5	23	1.06	8.3	6.0	1.5	–0.7	0.02–0.09	70
CB	olivine	<0.1	3.5	60–70	1.08	11.1	7.2	1.7	–1.4	0.5–5	30–40
Ordinary											
H	olivine	0.01–0.2	17	15–19	0.96	6.8	4.9	4.1	2.9	0.3	65–75
L	olivine	<0.1	22	4–9	0.93	6.6	4.7	4.6	3.5	0.7	65–75
LL	olivine	<0.1	27	0.3–3	0.94	6.5	4.7	4.9	3.9	0.9	65–75
Enstatite											
EH	enstatite	<0.1	0.05	8	0.73	5.0	3.6	5.6	3.0	0.2	60–80
EL	enstatite	<0.1	0.05	15	0.87	5.8	3.8	5.3	2.7	0.6	60–80
Other											
R	olivine	<0.1	38	<0.3	0.77	6.4	4.1	4.5	5.2	0.4	>40
K	enstatite	<0.1	2–4	6–10	0.95	6.9	5.0	2.7	–1.3	0.6	27

Wasson (1974), Table II-5. With kind permission of Springer Science+Business Media.

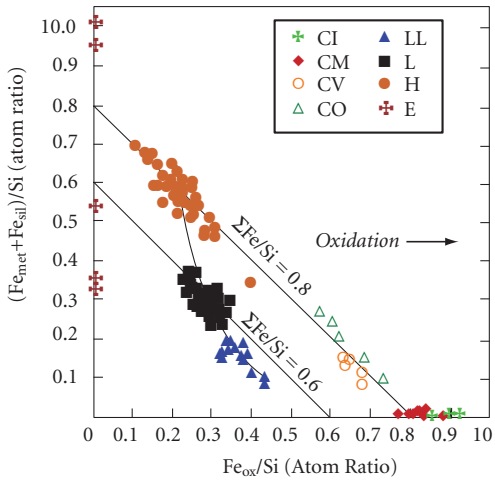

Figure 10.13 Ratio of reduced and oxidized iron to Si in chondrites. Carbonaceous and H group chondrites have approximately equal ΣFe/Si ratios; L and LL groups are iron-depleted. Wasson (1974). With kind permission of Springer Science+Business Media.

sphere. These compositions are also compared in Figure 10.14. As may be seen, the CI chondrite compositions match that of the Sun remarkably well for all but H, O, C, N, and the rare gases.* CI chondrites thus seem to be collections of bulk nebular dust that escaped the high-temperature processing and attendant chemical fractionations that affected material in other chondrites.

Because it matches the composition of the Sun so well, the composition of CI chondrites is taken to represent the composition of the solar system as a whole for the condensable elements. The terms *chondritic* and *solar composition* are thus effectively synonymous. You might ask why use the CI chondritic composition for the solar system when data for the composition of the Sun are available? The answer is that while the composition of the Sun can be determined spectrographically, this technique is not very accurate for trace elements, and, as we learned in Chapter 7, most elements are trace elements. Unfortunately, meteorites of this group are rare, likely a consequence of their fragile nature, and only one fall, *Orgueil* (which fell in the French town of that name in 1864) exists in enough quantity for complete and detailed chemical analysis.

In addition to these groups, there are two minor classes of chondrites, sometimes grouped together as "other chondrites". These include the R chondrites, of which there are only 19 known specimens. The R chondrites are so named for the type example *Rumuruti*, which fell in Kenya in 1934. The R chondrites are the opposite of the E chondrites in the sense that they are highly oxidized with practically no free metal. They typically contain fewer chondrules than ordinary chondrites and many are highly brecciated, suggesting they came from near the surface of their asteroid parent body. The K group consists of just 3 specimens. They are rich in the iron sulfide, troilite, show numerous primitive, armored chondrules, and have a unique chemical and oxygen isotope composition.

In addition to metal contents and oxidation state, the other compositional differences between chondrite classes are the concentrations of *refractory* elements and the concentrations of *volatile* elements. Let's pause here to define these terms. Si, Mg, and Fe are the most abundant condensable elements in chondrites. In a hot gas of solar composition, these three elements would condense at very similar temperatures (50% of the Si, Mg, and Fe would condense between 1340 and 1311 K at 0.1 Pa). Fifty percent of Al will condense at 1650 K, whereas 50% of Na will not condense until 970 K. We refer to elements that condense at higher temperature as *refractory* and elements that condense at lower temperature as *volatile*. This classification is sometimes further refined into moderately volatile, highly refractory, and so on. Figure 10.15 illustrates the compositional variation between chondrite classes for several lithophile elements, which are arranged going from most refractory (Al) to most volatile (Na). Concentrations are shown normalized both to Si and to CI chondrites. Thus Si plots at 1 for all classes, and CI chondrites would plot as a

* These elements will never fully condense from the solar nebula; instead large fractions will remain in the gas phase. These elements are thus termed *non-condensable*. Li is depleted in the Sun compared with chondrites because, as we saw, it is consumed in nuclear reactions in the Sun.

Table 10.2 Abundances of the elements.

Element		Solar system photosphere*	Concentration in *Orgueil* (CI)†	σ (%)	Element		Solar photosphere*	Concentration in *Orgueil* (CI)†	σ (%)
1	H	1×10^{12}	2.02%	10	44	Ru	69.2	0.683	3
2	He	9.77×10^{10}	56.0 nL/g		45	Rh	13.2	0.14	3
3	Li	1.26×10^{1}	1.49	10	46	Pd	49.0	0.556	10
4	Be	2.51×10^{1}	0.0249	10	47	Ag	8.71	0.197	10
5	B	5.01×10^{2}	0.69	13	48	Cd	58.9	0.68	10
6	C	2.45×10^{8}	3.22%	10	49	In	6.61	0.078	10
7	N	8.51×10^{7}	3180	10	50	Sn	1×10^{2}	1.68	10
8	O	4.90×10^{8}	46.4%	10	51	Sb	10	0.133	10
9	F	3.63×10^{4}	58.2	15	52	Te	1.72×10^{2}	2.27	10
10	Ne	1.00×10^{8}	203 pL/g		53	I	32.4	0.433	20
11	Na	2.14×10^{6}	4982	5	54	Xe	1.45×10^{2}	8.6 pL/g	
12	Mg	3.47×10^{7}	9.61%	3	55	Cs	13.2	0.188	5
13	Al	2.95×10^{6}	8490	3	56	Ba	1.35×10^{2}	2.41	10
14	Si	3.47×10^{7}	10.68%	3	57	La	14.8	0.245	5
15	P	2.82×10^{5}	926	7	58	Ce	38.0	0.639	5
16	S	2.14×10^{7}	5.41%	5	59	Pr	5.13	0.0964	10
17	Cl	3.16×10^{5}	698	15	60	Nd	31.6	0.474	5
18	Ar	2.51×10^{6}	751 pL/g		62	Sm	10.2	0.154	5
19	K	1.32×10^{5}	544	5	63	Eu	3.24	0.058	5
20	Ca	2.29×10^{6}	9320	3	64	Gd	13.2	0.204	5
21	Sc	1.48×10^{3}	5.90	3	65	Tb	0.79	0.0375	10
22	Ti	1.05×10^{5}	458	4	66	Dy	13.8	0.256	10
23	V	1.00×10^{4}	54.3	5	67	Ho	1.82	0.0567	10
24	Cr	4.68×10^{5}	2646	3	68	Er	8.51	0.166	5
25	Mn	2.45×10^{5}	1933	3	69	Tm	1.0	0.0256	10
26	Fe	2.82×10^{7}	18.43%	3	70	Yb	12.0	0.165	5
27	Co	8.32×10^{4}	506	3	71	Lu	1.15	0.0254	10
28	Ni	1.78×10^{6}	1.077%	3	72	Hf	7.59	0.107	5
29	Cu	1.62×10^{4}	131	10	73	Ta	0.74	0.0142	6
30	Zn	3.89×10^{4}	323	10	74	W	4.79	0.0903	4
31	Ga	7.59×10^{2}	9.71	5	75	Re	1.86	0.0395	4
32	Ge	1.57×10^{3}	32.6	10	76	Os	28.2	0.506	2
33	As	2.34×10^{2}	1.81	5	77	Ir	22.4	0.48	4
34	Se	2.24×10^{3}	21.4	5	78	Pt	63.1	0.982	4
35	Br	4.27×10^{2}	3.50	10	79	Au	10.2	0.148	4
36	Kr	2.0×10^{3}	8.7 pL/g		80	Hg	12.3	0.31	20
37	Rb	3.98×10^{2}	2.32	5	81	Tl	7.9	0.143	10
38	Sr	9.33×10^{2}	7.26	5	82	Pb	1.0×10^{2}	2.53	10
39	Y	1.74×10^{2}	1.56	3	83	Bi	5.31	0.111	15
40	Zr	3.98×10^{2}	3.86	2	90	Th	1.20	0.0298	10
41	Nb	26.3	0.247	3	92	U	3.39×10^{-1}	0.0078	10
42	Mo	83.2	0.928	5					

σ is the estimated uncertainty in the concentrations in CI chondrites.

* Atoms relative to H = 10^{12}.

† Concentrations in ppm unless otherwise indicated. Modified from Palme and Jones (2005). With permission from Elsevier.

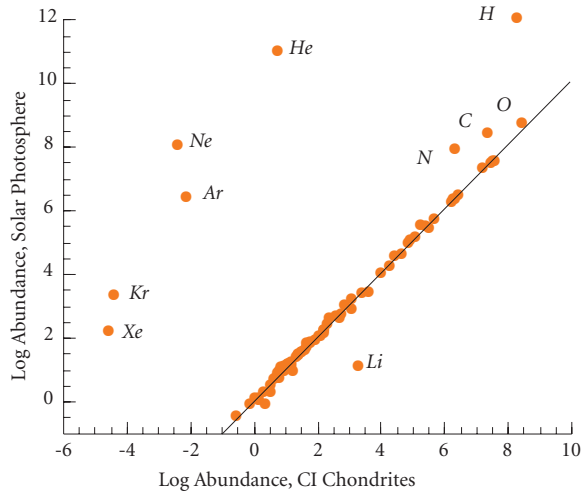

Figure 10.14 Abundances of the elements in the Sun's photosphere versus their abundances in the carbonaceous chondrite Orgueil (CI). Abundances for most elements agree within analytical error except non-condensing elements and Li.

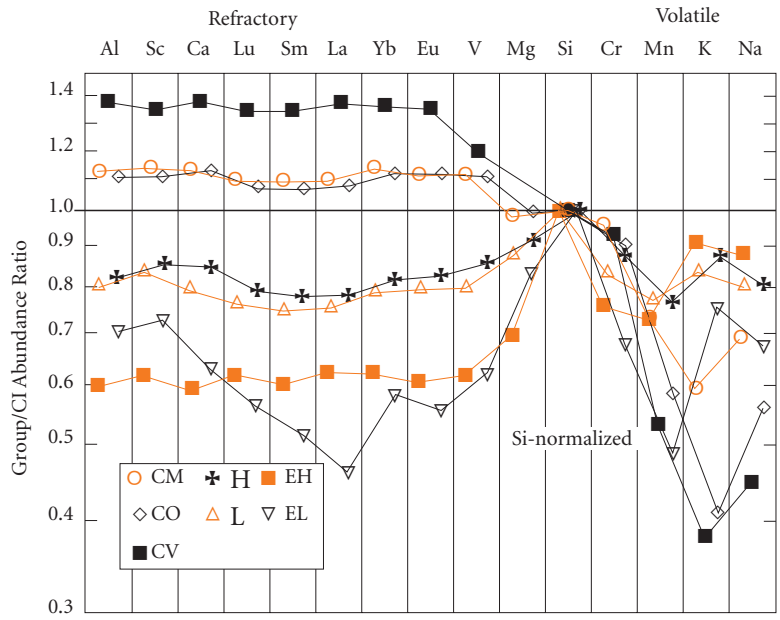

Figure 10.15 Silicon- and CI-normalized abundances of key elements in the main classes of chondrites. Elements are arranged from left to right in order of decreasing condensation temperature. Si concentration plots at 1 in each case. CI chondrites would plot as a horizontal line at 1. Wasson and Kallemeyn (1988). By permission of the Royal Society.

horizontal line at 1. We can see that all other chondrite groups are depleted in volatile elements compared with CI chondrites. We can also see that the other carbonaceous chondrites are enriched in refractory elements compared with CI chondrites, and ordinary and E chondrites are depleted in refractory elements compared with CI chondrites. Recalling that carbonaceous chondrites are enriched in the most volatile elements (H, C, N, etc. – not shown on this plot) compared with other chondrites, we realize that ordinary and

E chondrites are depleted in both the most refractory and the most volatile elements compared with CI chondrites. An interesting feature of this diagram is that despite variations in the absolute levels of refractory elements, the ratios of refractory elements to each other remain nearly constant across all chondrite classes except EL. This is an important observation generally taken as evidence that nebular processes were generally not able to fractionate the most refractory elements.

The compositional variations among chondrite classes illustrated in Figures 10.14 and 10.15 reflect variations in conditions in the solar nebula. Nevertheless, all meteorites have undergone subsequent processing on their parent bodies. Van Schmus and Wood (1967) devised a simple way to indicate the degree of parent body processing by dividing chondrites into petrologic types 1 through 6, based on increasing degree of metamorphism and decreasing volatile content. Types 1 and 2 have experienced low-temperature aqueous alteration, while types 4–6 have experienced increasingly high-temperature metamorphism. Type 3 objects have undergone the least parent body processing and are in this sense the most primitive. Table 10.3

Table 10.3 Van Schmus and Wood petrographic classification of chondrites (after Van Schmus and Wood, 1967). With permission from Elsevier.

	1	2	3	4	5	6
	Increasing temperature→					
Type	←Aqueous alteration			Thermal metamorphism →		
I. Olivine and pyroxene homogeneity		Greater than 5% mean deviation		Less than 5% mean deviation	Uniform	
II. Structural state of low-Ca pyroxene		Predominately monoclinic		Abundant monoclinic crystals	Orthorhombic	
III. Development of secondary feldspar		Absent		Predominately as microcrystalline aggregates		Clear, interstitial grains
IV. Igneous glass		Clear and isotropic primary glass; variable abundance		Turbid if present	Absent	
V. Metallic minerals (max. Ni content)		Taenite absent or minor (<20%)	Kamacite and taenite present (>20%)			
VI. Average Ni of sulfide minerals		>0.5%	<0.5%			
VII. Chondrules	No chondrules	Very sharply defined chondrules		Well-defined chondrules	Chondrules rarely seen	Poorly defined chondrules
VIII. Texture of matrix	All fine-grained	Much opaque matrix	Opaque matrix	Transparent microcrystalline matrix	Recrystallized matrix	
IX. Bulk carbon content	3–5%	0.8–2.6%	0.2–1%	<0.2%		
X. Bulk water content	18–22%	2–16%	0.3–3%	1.5%		

summarizes the Van Schmus and Wood classification scheme.

The petrologic types are used together with the above groups to classify meteorites as to origin and metamorphic grade, e.g., CV3. The petrologic type is correlated to a certain degree with chondrite class. Type 1 is restricted to CI, CM, and CR chondrites, and petrologic grades above 1 are not found among CI chondrites. Type 2 is restricted to CM and CR chondrites. Petrologic types 5 and 6 occur only in CK, ordinary, E, and R chondrites. Thermal metamorphism results in equilibration of the various minerals present in meteorites; consequently, petrologic types 4–6 are sometimes termed *equilibrated*, while those of low petrologic type are sometimes referred to as *unequilibrated*.

Chondrites can also be classified according to the degree of shock they have experienced. Class *S1* indicates no shock, class *S6* indicates very strong shock, with some shock melting present.

To gain a better understanding of what chondrites are and how they help us to understand the processes in the solar nebula, we briefly review the principal components of chondrites in the following sections.

10.3.1.2 Chondrules

Chondrules are usually a few tenths of a mm to a few mm in diameter (Figure 10.12). Mean size varies between chondrite classes (Table 10.1), but is typically around 0.5 mm. In the least metamorphosed meteorites, they consist of mixture of crystals and glass. Most are porphyritic, with relatively large olivine or pyroxene crystals in a fine-grained or glassy matrix. Non-porphyritic chondrules can consist of cryptocrystalline material or radial pyroxene or barred olivine, all of which suggest rapid crystallization. Olivine and Ca-poor pyroxene (enstatite, hypersthene) are by far the dominant minerals, with troilite (FeS), kamacite (FeNi alloy), Ca-rich pyroxene (pigeonite, diopside), Mg-Al spinel, chromite, and feldspar being less abundant. Some rare Al-rich chondrules have compositions similar to CAIs, which are discussed later. Some chondrules contain relict mineral grains and a few contain relict CAIs. Chondrules have remnant magnetism that was acquired as they cooled through their curie point in the presence of a magnetic field, indicating the presence of such a field in the solar nebula. From the number of compound chondrules (two chondrules fused together) and those having indentations suggestive of collisions with other chondrules, the chondrule density was as high as a few per m^3 at times and places in the solar nebula. While "dents" are observed in chondrules, microcraters produced by high-velocity impact are absent. Many chondrules are compositionally zoned, and most chondrules contain nuclei of relict crystals. Many are rimmed with fine-grained dark secondary coatings of volatile-rich material broadly similar in composition to the chondrite matrix.

Chondrules make up nearly half the mass, on average, of primitive meteorites. Therefore, understanding their origin is critical to understanding processes in the solar nebula because the dust in the nebula, which is the raw material for terrestrial planets, was apparently processed into chondrules. The presence of glass and their spheroidal shape indicates that chondrules represent melt droplets, as has been realized for at least 100 years. How these melts formed has been more difficult to understand. The main problem is that at the low pressures that must have prevailed in the solar nebula, liquids are not stable: solids should evaporate rather than melt. Chondrules seem to have been heated quite rapidly, at rates of 10^4 K/hr or more to peak temperatures of 1650 to 1850 K, and then cooled rapidly as well, at rates of 100–1000 K/hr. In most cases, peak temperatures were maintained for only minutes and they apparently cooled completely in hours to days. These inferences are based on compositional zonation of minerals and experimental reproduction of textures, strengthened by other experiments that show chondrules would have evaporated if they existed in the liquid state any longer than this. Though cooling was rapid, it was considerably slower than the rate that would have resulted from radiative cooling in open space. All these observations indicate they formed very quickly, and may never have reached equilibrium.

Over the past 100 years or so, many mechanisms for chondrule formation have been proposed. These include formation through volcanism on planets or asteroids, impact melting resulting from collisions of planets or planetesimals, condensation from hot nebular